Nano Research 2018, 11(3): 1238–1246
https://doi.org/10.1007/s12274-017-1737-6
Research Article

ISSN 1998-0124
CN 11-5974/O4

Hollow carbon nanofibers with dynamic adjustable pore sizes and closed ends as hosts for high-rate lithium-sulfur battery cathodes

Xiang-Qian Zhang, Bin He, Wen-Cui Li, and An-Hui Lu (✉)

State Key Laboratory of Fine Chemicals, School of Chemical Engineering, Faculty of Chemical, Environmental and Biological Science and Technology, Dalian University of Technology, Linggong Road 2, Dalian 116024, China

Received: 18 April 2017
Revised: 18 April 2017
Accepted: 22 June 2017

KEYWORDS
hollow carbon nanofibers,
pore-adjusting strategy,
sulfur cathodes,
rate capability,
energy materials

ABSTRACT

Designing a better carbon framework is critical for harnessing the high theoretical capacity of Li-S batteries and avoiding their drawbacks, such as the insulating nature of sulfur, active material loss, and the polysulfide shuttle reaction. Here, we report an ingenious design of hollow carbon nanofibers with closed ends and protogenetic mesopores in the shell that can be retracted to micropores after sulfur infusion. Such dynamic adjustable pore sizes ensure a high sulfur loading, and more importantly, eliminate excessive contact of sulfur species with the electrolyte. Together, the high aspect ratio and thin carbon shells of the carbon nanofibers facilitate rapid transport of Li^+ ions and electrons, and the closed-end structure of the carbon nanofibers further blocks polysulfide dissolution from both ends, which is remarkably different from that for carbon nanotubes with open ends. The obtained sulfur-carbon cathodes exhibit excellent performance marked by high sulfur utilization, superior rate capability (1,170, 1,050, and 860 $mA{\cdot}h{\cdot}g^{-1}$ at 1.0, 2.0, and 4.0 C (1 C = 1.675 $A{\cdot}g^{-1}$), respectively), and a stable reversible capacity of 847 $mA{\cdot}h{\cdot}g^{-1}$ after 300 cycles at a high rate of 2.0 C.

1 Introduction

Nanostructured carbons with abundant porosity, good conductivity, chemical stability, and tunable morphologies are attractive as conducting and confining hosts for insulative or poor electroconductive active materials (e.g., sulfur, metal oxides) in lithium secondary batteries [1–4]. The introduction of carbons can improve the conductivity and relieve the volume variations of electroactive materials during charge–discharge possesses, by which the rate performance and long cycle stability can be enhanced [5–8]. As a good example, using carbon as the sulfur host for Li-S batteries can fully encapsulate the advantages of carbon and, in principle, complement the inherent drawbacks of sulfur cathodes [9–11]. Nazar's group

Address correspondence to anhuilu@dlut.edu.cn

pioneered this area by creating an ordered mesoporous carbon framework to encapsulate sulfur species within resident nanochannels, which greatly accelerated the electrochemical reaction kinetics [12]. Thereafter, numerous nanocarbons with various morphologies and pore structures have been prepared, including micro/mesoporous carbons [13–17], hollow carbon fibers [18, 19], carbon nanotubes [20–23], and graphene nanosheets [24–26].

Mesoporous and macroporous carbons provide sufficient space for efficient sulfur loading and volume expansion compensation during lithiation and delithiation [27–30]. However, the sulfur species located in these "open-type" carbons are easily accessed by the electrolyte, which often couples with a severe shuttle problem and undermines the cycling performance. These problems also plague carbon nanotubes and hollow carbon fibers with open ends, which can potentially become pathways for polysulfide dissolution [3, 18, 31]. Decreasing the pore sizes to the microporous scale is helpful to restrain polysulfide diffusion through the physical barrier that prevents contact between the polysulfide intermediates and the organic electrolyte [14, 20, 32]. Yet, the limited pore volumes limit the sulfur loading content [3, 20, 33]. To solve these problems, Huang and co-workers synthesized a core–shell carbon with an ordered mesoporous core and microporous shell for stable storage of the sulfur species [34]. However, the rate performance is not satisfactory because of the sluggish mass transfer caused by the overall large sizes (> 1 μm) and thick microporous shells (> 80 nm).

Therefore, the remaining challenge is to reasonably design novel nanostructured carbon hosts. A large space is necessary to ensure a high loading of active materials, and a short mass transport path should be available to obtain a high rate performance [18, 30]. Under this consideration, one-dimensional (1D) hollow carbon nanofibers (HCFs) with a high aspect ratio and nanosized diameter are expected to act as a conductive network [18, 19]. To suppress the shuttle problem with the guarantee of easy immersion of active sulfur, the pore sizes can be adjusted from macropores or mesopores to micropores after sulfur storage. Until now, the above-mentioned carbons have not been obtained. The major difficulty is to dynamically adjust the pore sizes of the carbons because the reported carbons are mostly obtained by high-temperature pyrolysis; once the carbon skeleton is formed, the porosity is stationary and cannot be initiatively altered.

In this work, we propose a rational design for 1D HCFs with dynamic adjustable pore sizes and two closed ends as a sulfur host for Li-S battery cathodes. Such fibrous carbons can construct a conducting and robust network; meanwhile, they provide a short transport path for Li^+ ions and electrons. The small spaces render the formation of nanosized electroactive sulfur particles that can implement a superb performance at high rates. The initially formed mesopores on the shell facilitate easy access of active materials into the interior, and the subsequent narrowed microporous shell (pore size = 0.58 nm) and closed ends minimize the sulfur-electrolyte contact area, which ensures effective polysulfide confinement. With the favorable structure, the prepared S@HCF cathodes demonstrate a high initial capacity of 1,264 $mA{\cdot}h{\cdot}g^{-1}$ at 0.5 C (1 C = 1.675 $A{\cdot}g^{-1}$), substantial capacity retention over 500 cycles (2.0 C), and excellent rate capability of 860 $mA{\cdot}h{\cdot}g^{-1}$ at a high rate of 4.0 C.

2 Experimental

2.1 Chemicals

Resorcinol (99.5%), hexamethylenetetramine, cetyltrimethyl-ammonium bromide (99%), tetraethyl orthosilicate, ammonia solution (25%), and hydrofluoric acid (HF) were obtained from Sinopharm Chemical Reagent Co., Ltd. Pluronic F127 was purchased from Fluka. Sulfur (> 99.99%) was purchased from Aldrich. Ketjen Black carbon was purchased from Shanghai Changxiang Trade Co., Ltd. All chemicals were used as received.

2.2 Synthesis of hollow carbon nanofibers as a sulfur host

The preparation process for the hollow carbon fibers for use in sulfur cathodes is shown in Fig. 1. In detail, resorcinol-formaldehyde resin polymer nanofibers (PFs) were prepared as a carbon precursor according to a modified method reported by our group [35].

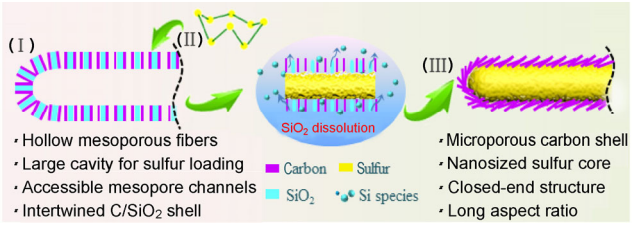

Figure 1 Schematic illustration for the preparation of HCFs with adjustable pore sizes as the sulfur host.

Then, a layer of silica was uniformly coated onto the surface of the PF fibers through a modified Stöber method, generating PF@SiO_2 fibers. HCF/SiO_2 was obtained by pyrolyzing the above PF@SiO_2 at 600 ℃ for 2 h under an argon flow. Then, the as-prepared HCF/SiO_2 and a certain amount of sulfur (the mass ratio of sulfur to HCF/SiO_2 is ~ 2.3) were ground together, heated to 155 ℃ and maintained for 10 h to facilitate sulfur diffusion into the porous host, and treated at 300 ℃ under an argon flow for ~ 0.5 h to optimize the sulfur content. Finally, S@HCF was obtained by using an 8.2 M HF solution to dissolve the silica at room temperature overnight. HCF was obtained by volatizing sulfur in S@HCF at 500 ℃ for 2 h under an argon flow.

2.3 Synthesis of the sulfur/Ketjen Black carbon (S/KC) composite

The S/KC composite was synthesized by a melting-diffusion strategy. Sulfur (0.3 g) was well mixed with 0.2 g of Ketjen Black carbon. The mixture was heated to 155 ℃ and maintained for 10 h to facilitate sulfur diffusion into the porous host.

2.4 Characterizations

Scanning electron microscopy (SEM) and energy-dispersive X-ray spectroscopy (EDX) were performed using an FEI Nova NanoSEM 450 instrument. Transmission electron microscopy (TEM) analyses were carried out with an FEI Tecnai G220S-Twin instrument. Thermogravimetric analysis was conducted on a NETZSCH STA 449 F3 thermogravimetric analyzer under a nitrogen flow. The nitrogen sorption isotherms were measured with a Micromeritics ASAP 2020 adsorption analyzer at −196 ℃. Before the measurements, all samples were degassed at 200 ℃ for 6 h. The total pore volume (V_{total}) was estimated from the amount adsorbed at a relative pressure of 0.99. Pore size distributions were determined from the adsorption branch of the isotherm using density functional theory. X-ray powder diffraction (XRD) was carried out on a PANalytical X'Pert X-ray diffractometer equipped with graphite-monochromatized Cu Kα radiation.

2.5 Electrochemical characterizations

Electrochemical experiments were performed using CR2025 coin-type test cells assembled in an argon-filled glovebox with lithium metal as the counter and reference electrodes at room temperature. The cathode for the Li-S batteries was prepared by mixing 75 wt.% carbon-sulfur composites, 15 wt.% carbon black (Super P), and 10 wt.% polyvinylidenedifluoride in N-methyl-2-pyrrolidone to form a slurry that was pasted onto a carbon-coated aluminum foil. The mass loading of the active material (sulfur) was approximately 1.5 mg·cm^{-2}. A Celgard 2400 membrane was used as the separator. The electrolyte was 1 M bis(trifluoromethane) sulfonimide lithium salt dissolved in a mixture of 1,3-dioxolane and dimethoxymethane (1:1, *v*/*v*) containing 0.2 M $LiNO_3$, and 20 μL was used for each cell. Considering the low potential value (< 1.6 V) of $LiNO_3$ decomposition [36], the discharge–charge tests were conducted between 1.7 and 2.8 V using a Land CT2001A battery test system. The capacity values were calculated based on the sulfur mass, unless otherwise stated. Cyclic voltammograms (CVs) were measured with a CHI 660D electrochemical workstation (Shanghai Chenhua Instrument Co., Ltd.) at a scan rate of 0.2 mV·s^{-1}. Electrochemical impedance spectroscopy (EIS) was carried out in the range of 100 kHz to 10 mHz on the CHI 660D workstation.

3 Results and discussion

Figure 1 shows the preparation process of the hollow carbon fibers with adjustable pore sizes (mesopores to micropores) as the host material by a silica-assisted approach, which includes (I) synthesis of hollow HCF/SiO_2 fibers with protogenetic mesoporous shells (Fig. 2(a), the synthesis details are supplied in the Experimental section), (II) active materials loading

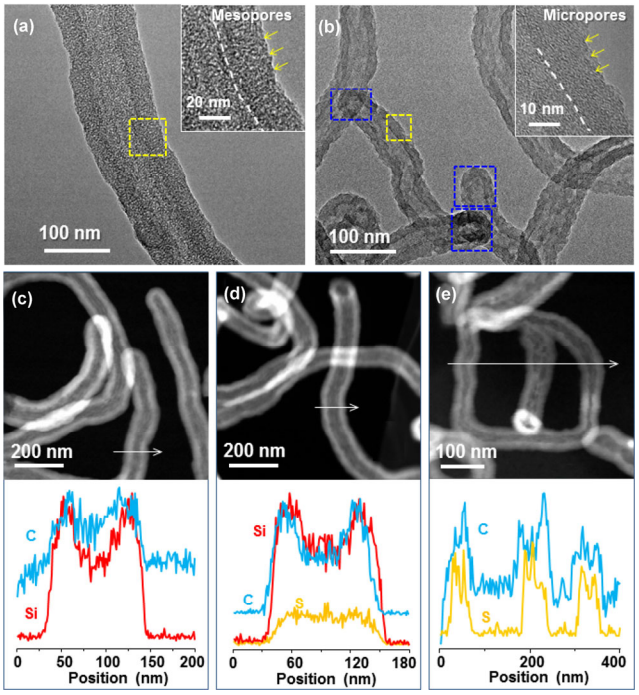

Figure 2 (a) TEM images of HCF/SiO_2 displaying the cavity and mesoporous shell. (b) TEM images of S@HCF; the inset shows the microporous shell. STEM images and linear EDX element distributions of (c) HCF/SiO_2, (d) sulfur/HCF/SiO_2, and (e) S@HCF.

(here, sulfur is used), and (III) SiO_2 dissolution to form S@HCF with a micrporous shell (Fig. 2(b)). During the process, SiO_2 initially acts as an upholder to keep the mesopores in the thin carbon shell stable, thus facilitating a sulfur infusion into the interior space. Subsequently, SiO_2 is gradually dissolved in the HF solution, and then the carbon matrices tend to stack close together to minimize the surface energy. As a result, the mesopores in the carbon shell are tuned into micropores, and the sulfur is stably settled in the interior of HCF. Such an ingenious SiO_2-assisted pore adjusting method is reported for the first time toward advanced sulfur-carbon cathodes.

TEM images (Fig. 2(a) and Fig. S1 in the Electronic Supplementary Material (ESM)) show that the HCF/SiO_2 composites exhibit a hollow fibrous structure with a cavity of ~ 40 nm in diameter and abundant mesopore channels on the shell. The nitrogen sorption isotherm of HCF/SiO_2 is a type-IV isotherm with a hysteresis loop (Fig. S2 in the ESM), further indicating the mesoporous characteristics with a pore size of ~ 2.34 nm and a specific surface area (S_{BET}) of 809 $m^2 \cdot g^{-1}$, which can provide accessible space and pathways for sulfur infusion. Scanning transmission electron microscopy (STEM) and EDX studies were conducted to observe the structural evolution and elemental distribution of samples obtained during the synthetic process. Figure 2(c) shows a homogeneous distribution of C and Si elements in the shell, confirming the intertwined carbon matrix with SiO_2 in HCF/SiO_2. After sulfur infusion, the linear EDX elemental distributions of S, C, and Si (Fig. 2(d)) demonstrate that most of the sulfur is confined in the cavity of HCF/SiO_2, which is crucial to keep the "sulfur core" stable in the fiber during the following treatment. Finally, the S@HCF composite was obtained after etching the silica. The linear EDX elemental distributions of S and C (Fig. 2(e)) confirm that the distribution of S is contrary to that of C, demonstrating a core@shell structure with sulfur mainly confined in the cavity of HCF by the carbon shell. The TEM image (Fig. 2(b)) demonstrates the fiber morphology of S@HCF with inner and outer diameters of approximately 30 and 60 nm, respectively. The blue dashed box in Fig. 2(b) highlights the closed ends of HCF, which ensure the fine confinement of sulfur stored in the cavity. Moreover, as indicated by the HRTEM image (Fig. 2(b) inset) and N_2 sorption measurement (Fig. S2 in the ESM), the carbon shell is tailored to micropores with a S_{BET} of 551 $m^2 \cdot g^{-1}$. Notably, the micropores (~0.58 nm) of the carbon shell in HCF are smaller than the lithium polysulfides (Li_2S_x, $x \geq 4$); thus, they are potentially well suited as physical barriers to prevent polysulfide diffusion while still allowing transport of Li^+ ions and electrons [34, 37].

The SEM images (Figs. 3(a) and 3(b)) show that the composites maintain their fibrous shape and are closely stacked, which is favorable for forming a good electronically conductive network [38]. The presence of sulfur and its uniform distribution over a large area is also confirmed by SEM-equipped EDX analysis (Fig. S3 in the ESM). The XRD pattern (Fig. 3(c)) of the S@HCF exhibits much weaker diffraction of sulfur, also indicating the excellent confinement of sulfur inside the HCF. The sulfur content is ~ 61 wt.% (by thermogravimetric analysis, Fig. 3(d)).

The electrochemical performance of the S@HCF composite was evaluated and is presented in Fig. 4.

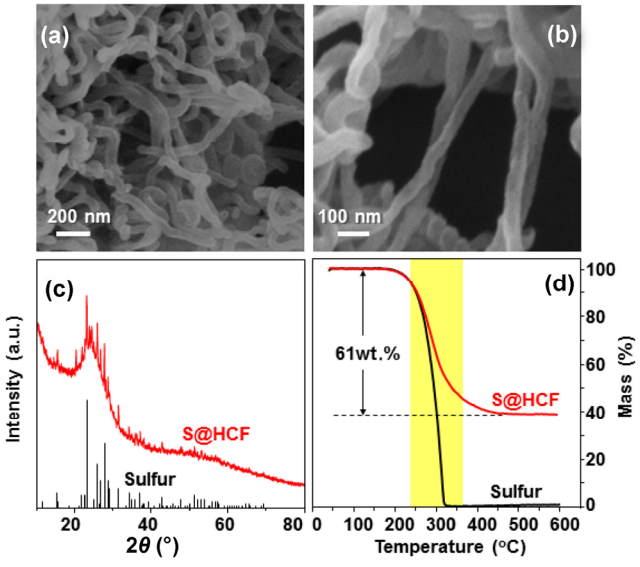

Figure 3 (a) and (b) SEM images of S@HCF. (c) XRD patterns and (d) TG curves of S@HCF and sulfur powder under a N_2 atmosphere.

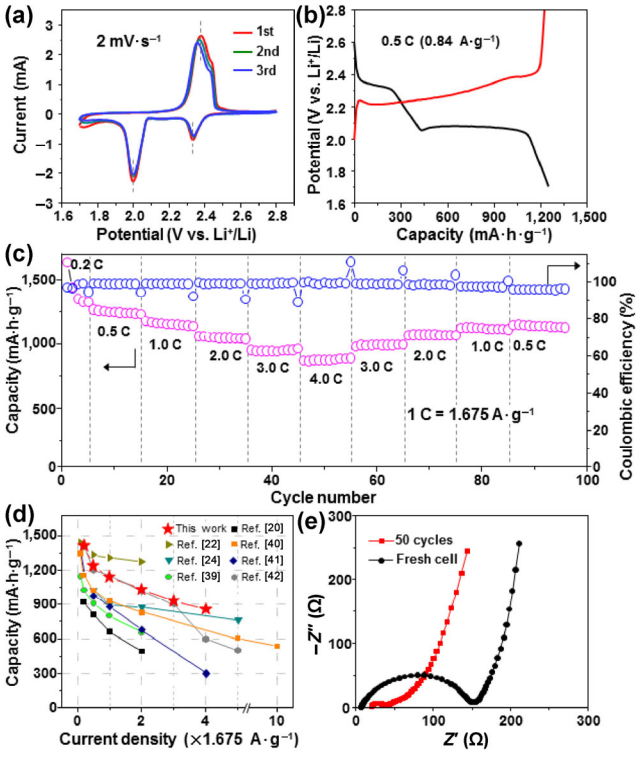

Figure 4 Electrochemical performance of the S@HCF composite. (a) The CV at a scan rate of 0.2 $mV·s^{-1}$ for the first three cycles. (b) The galvanostatic charge/discharge potential profiles for the first cycle at a current density of 0.5 C (0.84 $A·g^{-1}$). (c) Discharge capacities and coulombic efficiency at various rate capabilities from 0.2 to 4.0 C. (d) Rate capabilities of the S@HCF cathodes in this work compared with other carbon hosts reported in the literature. (e) EIS of the S@HCF cathode before and after the cycling test.

The CVs (Fig. 4(a)) demonstrate two typical cathodic peaks of the Li-S cells at 2.33 and 2.0 V, corresponding to the reduction of elemental sulfur to high-order polysulfides and further reduction to lower order polysulfides, respectively [13, 20]. The anodic peak observed at 2.37 V is attributed to the conversion of lithium sulfides to sulfur [13]. The redox peaks in the following cycles almost overlap, indicating an excellent reversibility of the composites. In the initial charge/discharge potential profiles at a 0.5 C rate (1 C = 1.675 $A·g^{-1}$) (Fig. 4(b)), the discharge curve displays two typical plateaus, in agreement with the cathodic peaks in the CV. Moreover, the second plateau is flat, suggesting a uniform deposition of Li_2S with minimal kinetic barriers [18]. A high discharge capacity of 1,264 $mA·h·g^{-1}$ is achieved, indicating a high utilization of sulfur. This could be attributed to the unique structures of HCF with a small inner diameter and thin carbon shell, which significantly improves the electronic and ionic transport at the cathode.

The S@HCF cathode presents a high rate capability and good electrode kinetics, as shown in Fig. 4(c) and Fig. S4 in the ESM. The discharge capacity shows a small steady decrease as the current rate increases from 0.2 to 4.0 C. In the first cycle at 0.2 C, the discharge capacity of S@HCF is 1,638 $mA·h·g^{-1}$, corresponding to 98% of the theoretical capacity of sulfur. After 5 cycles at 0.2 C, the S@HCF electrode delivers high coulombic efficiencies and high stabilized specific capacities of 1,264, 1,170, 1,050, 935, and 860 $mA·h·g^{-1}$ at 0.5, 1.0, 2.0, 3.0, and 4.0 C, respectively, which exceed or are on par with that of most reported sulfur-carbon cathodes (Fig. 4(d)) [15, 24, 39–42]. When the current density is switched back to 0.5 C, most of the original capacity is recovered. Further, the SEM and TEM images (Fig. S5 in the ESM) of S@HCF after cycling show that the fibrous morphology is retained, indicating the good stability of the cathode structure after the high rate test. The EIS data in Fig. 4(e) show that the resistance of the cell obtained after the cycles is lower than that of the fresh cell, which is mainly attributed to the electrolyte gradually penetrating the S@HCF structures during the initial cycles, thus decreasing the charge transfer resistance at the interface of the active materials and electrolyte [43, 44]. These results consolidate our expectation that the as-prepared

S@HCF materials could preserve the rapid Li^+ ions and electron transportation kinetics for a prominent high-rate performance.

Figure 5 shows the cycling performances of S@HCF and the contrast sample (S/KC) that uses the commercially available mesoporous carbon as a host with a sulfur content of 60 wt.%. As can be observed, S@HCF delivers a high initial discharge capacity of 1,197 $mA·h·g^{-1}$ and retains a capacity of 1,012 $mA·h·g^{-1}$ after 100 cycles at a current rate of 1.0 C (Fig. 5(a)). The Coulombic efficiency of the battery is close to 100% throughout the cycles, indicating the fine accommodation of sulfur species inside the carbon host. In comparison, the S/KC electrode exhibits a severe capacity fading. The initial capacity is 1,056 $mA·h·g^{-1}$ at 1.0 C, which rapidly decreases to 688 $mA·h·g^{-1}$ after only 50 cycles and may be caused by the loss of active materials through polysulfide dissolution and diffusion in the electrolyte. To confirm this, the separators of both cells were examined (inset in Fig. 5(a)). The separator from the S@HCF cell shows a slight coloring, indicating the efficient confinement of sulfur species inside HCF by the microporous carbon shell. In contrast, the color on the separator of S/KC is more distinct, implying that significant amounts of polysulfides are dissolved from the mesoporous S/KC cathodes during cycling.

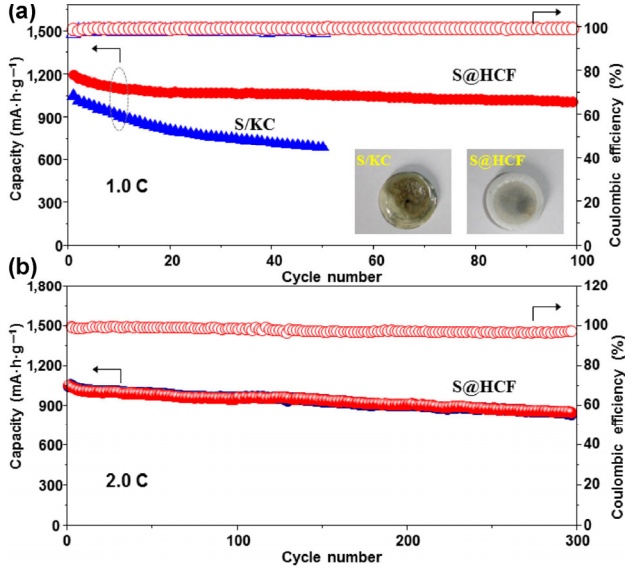

Figure 5 (a) Cycling performance and digital photos of cycled separators of the S@HCF and S/KC (contrast sample) after 100 cycle tests. (b) Prolonged cycling performance and the corresponding coulombic efficiency of S@HCF at a high rate of 2.0 C.

The prolonged cycle life of the S@HCF electrode was identified at a high rate of 2.0 C. After an activation process during the first several cycles, the electrode delivers high reversible capacities of 847 and 620 $mA·h·g^{-1}$ after 300 and 500 cycles (Fig. 5(b) and Fig. S6 in the ESM), demonstrating a relatively low capacity decay of 0.055% and 0.078% per cycle, respectively. The average Coulombic efficiency of the battery is > 98% throughout the long-term cycles, indicating a highly reversible and stable electrochemistry in the S@HCF electrode, which are superior to many carbon-sulfur materials reported previously (Table S1 in the ESM) [20, 23, 45–47]. Further, to verify the advantages of the SiO_2-assisted sulfur infusion strategy, S/microporous carbon fibers with identical sulfur contents (65 wt.%) were prepared by the traditional sulfur impregnation strategy [35]. The electrochemical test result (Fig. S7 in the ESM) shows that the obtained sulfur/carbon composite exhibits a capacity of 681 $mA·h·g^{-1}$ at 0.5 C after the first five activation cycles. However, it rapidly decreases and only remains at 434 $mA·h·g^{-1}$ after 200 cycles, which is significantly lower than that of S@HCF (910 $mA·h·g^{-1}$) at a higher current density of 2.0 C. Above all, such a supreme performance of the S@HCF electrodes is attributed to (1) the 1D fibers closely stack together forming a conductive network and providing short-range Li^+ ion and electron transport paths, promising a high sulfur utilization and good rate capability; (2) the cavity of the hollow materials allows a high loading of sulfur and accommodates the large volumetric expansion of sulfur during the lithiation/delithiation processes; (3) a closed-end structure together with the microporous carbon shell efficiently hinders the dissolution and diffusion of polysulfides, rendering a stable cycle life.

4 Conclusions

We developed an ingenious design for HCFs with closed ends and dynamic adjustable pore sizes for loading electrochemically active species. Using sulfur as an example of an active material, the obtained fibers have a high aspect ratio, thin carbon shells, and a closed-end structure, which together facilitates

the rapid transport of Li^+ ions and electrons while avoiding the higher exposure of sulfur species to the electrolyte, thus mitigating polysulfide dissolution. As a result, the obtained S@HCF cathode delivers a high sulfur utilization of up to 98%, high specific capacity of 860 $mA{\cdot}h{\cdot}g^{-1}$ at 4.0 C, and an excellent cycling stability, e.g., 847 and 620 $mA{\cdot}h{\cdot}g^{-1}$ at 2.0 C after 300 and 500 cycles, respectively. This carbon structure may allow for the introduction of other functional components into their interiors for use in batteries, catalysis, and so on.

Acknowledgements

This work was supported by the National Basic Research Program of China (No. 2013CB934104), the National Natural Science Foundation of China (Nos. 21225312 and 21376047), and Cheung Kong Scholars Program of China (No. T2015036).

Electronic Supplementary Material: Supplementary material (further details of the SEM, TEM images, and prolonged cycling performance of S@HCF, etc.) is available in the online version of this article at https://doi.org/10.1007/s12274-017-1737-6.

References

[1] Yang, Y.; Zheng, G. Y.; Cui, Y. Nanostructured sulfur cathodes. *Chem. Soc. Rev.* **2013**, *42*, 3018–3032.

[2] Wang, L. N.; Wang, Y. G.; Xia, Y. Y. A high performance lithium-ion sulfur battery based on a Li_2S cathode using a dual-phase electrolyte. *Energy Environ. Sci.* **2015**, *8*, 1551–1558.

[3] Li, Z.; Huang, Y. M.; Yuan, L. X.; Hao, Z. X.; Huang, Y. H. Status and prospects in sulfur–carbon composites as cathode materials for rechargeable lithium–sulfur batteries. *Carbon* **2015**, *92*, 41–63.

[4] Dai, L. M.; Chang, D. W.; Baek, J. B.; Lu, W. Carbon nanomaterials for advanced energy conversion and storage. *Small* **2012**, *8*, 1130–1166.

[5] Borchardt, L.; Oschatz, M.; Kaskel, S. Carbon materials for lithium sulfur batteries—Ten critical questions. *Chem.—Eur. J.* **2016**, *22*, 7324–7351.

[6] Wang, J. L.; He, Y. S.; Yang, J. Sulfur-based composite cathode materials for high-energy rechargeable lithium batteries. *Adv. Mater.* **2015**, *27*, 569–575.

[7] Chen, S. Q.; Sun, B.; Xie, X. Q.; Mondal, A. K.; Huang, X. D.; Wang, G. X. Multi-chambered micro/mesoporous carbon nanocubes as new polysulfides reserviors for lithium–sulfur batteries with long cycle life. *Nano Energy* **2015**, *16*, 268–280.

[8] Zheng, Z. M.; Guo, H. C.; Pei, F.; Zhang, X.; Chen, X. Y.; Fang, X. L.; Wang, T. H.; Zheng, N. F. High sulfur loading in hierarchical porous carbon rods constructed by vertically oriented porous graphene-like nanosheets for Li–S batteries. *Adv. Funct. Mater.* **2016**, *26*, 8952–8959.

[9] Yin, Y. X.; Xin, S.; Guo, Y. G.; Wan, L. J. Lithium–sulfur batteries: Electrochemistry, materials, and prospects. *Angew. Chem., Int. Ed.* **2013**, *52*, 13186–13200.

[10] Bruce, P. G.; Freunberger, S. A.; Hardwick, L. J.; Tarascon, J. M. $Li–O_2$ and Li–S batteries with high energy storage. *Nat. Mater.* **2012**, *11*, 19–29.

[11] Chen, H. W.; Wang, C. H.; Dong, W. L.; Lu, W.; Du, Z. L.; Chen, L. W. Monodispersed sulfur nanoparticles for lithium–sulfur batteries with theoretical performance. *Nano Lett.* **2015**, *15*, 798–802.

[12] Ji, X. L.; Lee, K. T.; Nazar, L. F. A highly ordered nanostructured carbon–sulphur cathode for lithium–sulphur batteries. *Nat. Mater.* **2009**, *8*, 500–506.

[13] Jayaprakash, N.; Shen, J.; Moganty, S. S.; Corona, A.; Archer, L. A. Porous hollow carbon@sulfur composites for high-power lithium–sulfur batteries. *Angew. Chem., Int. Ed.* **2011**, *123*, 6026–6030.

[14] Zhang, B.; Qin, X.; Li, G. R.; Gao, X. P. Enhancement of long stability of sulfur cathode by encapsulating sulfur into micropores of carbon spheres. *Energy Environ. Sci.* **2010**, *3*, 1531–1537.

[15] Zhou, W. D.; Wang, C. M.; Zhang, Q. L.; Abruña, H. D.; He, Y.; Wang, J. W.; Mao, S. X.; Xiao, X. C. Tailoring pore size of nitrogen-doped hollow carbon nanospheres for confining sulfur in lithium–sulfur batteries. *Adv. Energy Mater.* **2015**, *5*, 1401752.

[16] Sun, Q.; He, B.; Zhang, X.-Q.; Lu, A.-H. Engineering of hollow core–shell interlinked carbon spheres for highly stable lithium–sulfur batteries. *ACS Nano* **2015**, *9*, 8504–8513.

[17] Peng, X.-X.; Lu, Y.-Q.; Zhou, L.-L.; Sheng, T.; Shen, S.-Y.; Liao, H.-G.; Huang, L.; Li, J.-T.; Sun, S.-G. Graphitized porous carbon materials with high sulfur loading for lithium–sulfur batteries. *Nano Energy* **2017**, *32*, 503–510.

[18] Zheng, G. Y.; Yang, Y.; Cha, J. J.; Hong, S. S.; Cui, Y. Hollow carbon nanofiber-encapsulated sulfur cathodes for high specific capacity rechargeable lithium batteries. *Nano Lett.* **2011**, *11*, 4462–4467.

[19] Li, Z.; Zhang, J. T.; Lou, X. W. Hollow carbon nanofibers filled with MnO_2 nanosheets as efficient sulfur hosts for lithium–sulfur batteries. *Angew. Chem., Int. Ed.* **2015**, *54*, 12886–12890.

[20] Mi, K.; Jiang, Y.; Feng, J. K.; Qian, Y. T.; Xiong, S. L. Hierarchical carbon nanotubes with a thick microporous wall and inner channel as efficient scaffolds for lithium–sulfur batteries. *Adv. Funct. Mater.* **2016**, *26*, 1571–1579.

[21] Hu, G. J.; Sun, Z. H.; Shi, C.; Fang, R. P.; Chen, J.; Hou, P. X.; Liu, C.; Cheng, H. M.; Li, F. A sulfur-rich copolymer@CNT hybrid cathode with dual-confinement of polysulfides for high-performance lithium–sulfur batteries. *Adv. Mater.* **2017**, *29*, 1603835.

[22] Jin, F. Y.; Xiao, S.; Lu, L. J.; Wang, Y. Efficient activation of high-loading sulfur by small CNTs confined inside a large CNT for high-capacity and high-rate lithium–sulfur batteries. *Nano Lett.* **2016**, *16*, 440–447.

[23] Zhao, Y.; Wu, W. L.; Li, J. X.; Xu, Z. C.; Guan, L. H. Encapsulating MWNTs into hollow porous carbon nanotubes: A tube-in-tube carbon nanostructure for high-performance lithium–sulfur batteries. *Adv. Mater.* **2014**, *26*, 5113–5118.

[24] Zhang, J.; Yang, C.-P.; Yin, Y.-X.; Wan, L.-J.; Guo, Y.-G. Sulfur encapsulated in graphitic carbon nanocages for high-rate and long-cycle lithium–sulfur batteries. *Adv. Mater.* **2016**, *28*, 9539–9544.

[25] Pang, Q.; Kundu, D.; *Nazar*, L. F. A graphene-like metallic cathode host for long-life and high-loading lithium–sulfur batteries. *Mater. Horiz.* **2016**, *3*, 130–136.

[26] Zhou, G. M.; Pei, S. F.; Li, L.; Wang, D.-W.; Wang, S. G.; Huang, K.; Yin, L.-C.; Li, F.; Cheng. H.-M. A graphene–pure-sulfur sandwich structure for ultrafast, long-life lithium–sulfur batteries. *Adv. Mater.* **2014**, *26*, 625–631.

[27] He, B.; Li, W.-C.; Yang, C.; Wang, S.-Q.; Lu, A.-H. Incorporating sulfur inside the pores of carbons for advanced lithium–sulfur batteries: An electrolysis approach. *ACS Nano* **2016**, *10*, 1633–1639.

[28] Zhou, W. D.; Xiao, X. C.; Cai, M.; Yang, L. Polydopamine-coated, nitrogen-doped, hollow carbon–sulfur double-layered core–shell structure for improving lithium–sulfur batteries. *Nano Lett.* **2014**, *14*, 5250–5256.

[29] Zhou, W. D.; Yu, Y. C.; Chen, H.; DiSalvo, F. J.; Abruña, H. D. Yolk–shell structure of polyaniline-coated sulfur for lithium–sulfur batteries. *J. Am. Chem. Soc.* **2013**, *135*, 16736–16743.

[30] Zhou, Y.; Zhou, C. G.; Li, Q. Y.; Yan, C. J.; Han, B.; Xia, K. S.; Gao, Q.; Wu, J. P. Enabling prominent high-rate and cycle performances in one lithium–sulfur battery: Designing permselective gateways for Li^+ transportation in holey-CNT/S cathodes. *Adv. Mater.* **2015**, *27*, 3774–3781.

[31] Chen, S. Q.; Huang, X. D.; Liu, H.; Sun, B.; Yeoh, W.; Li, K. F.; Zhang, J. Q.; Wang, G. X. 3D hyperbranched hollow carbon nanorod architectures for high-performance lithium–sulfur batteries. *Adv. Energy Mater.* **2014**, *4*, 1301761.

[32] Li, Z.; Yuan, L. X.; Yi, Z. Q.; Sun, Y. M.; Liu, Y.; Jiang, Y.; Shen, Y.; Xin, Y.; Zhang, Z. L.; Huang, Y. H. Insight into the electrode mechanism in lithium-sulfur batteries with ordered microporous carbon confined sulfur as the cathode. *Adv. Energy Mater.* **2014**, *4*, 1301473.

[33] Zhu, Q. Z.; Zhao, Q.; An, Y. B.; Anasori, B.; Wang, H. R.; Xu, B. Ultra-microporous carbons encapsulate small sulfur molecules for high performance lithium–sulfur battery. *Nano Energy* **2017**, *33*, 402–409.

[34] Li, Z.; Jiang, Y.; Yuan, L. X.; Yi, Z. Q.; Wu, C.; Liu, Y.; Strasser, P.; Huang, Y. H. A highly ordered meso@microporous carbon-supported sulfur@smaller sulfur core–shell structured cathode for Li–S batteries. *ACS Nano* **2014**, *8*, 9295–9303.

[35] Zhang, X.-Q.; Sun, Q.; Dong, W.; Li, D.; Lu, A.-H.; Mu, J.-Q.; Li, W.-C. Synthesis of superior carbon nanofibers with large aspect ratio and tunable porosity for electrochemical energy storage. *J. Mater. Chem. A* **2013**, *1*, 9449–9455.

[36] de Godoi, F. C.; Wang, D.-W.; Zeng, Q. C.; Wu, K.-H.; Gentle, I. R. Dependence of $LiNO_3$ decomposition on cathode binders in Li–S batteries. *J. Power Sources* **2015**, *288*, 13–19.

[37] Li, C. Y.; Ward, A. L.; Doris, S. E.; Pascal, T. A.; Prendergast, D.; Helms, B. A. Polysulfide-blocking microporous polymer membrane tailored for hybrid Li-sulfur flow batteries. *Nano Lett.* **2015**, *15*, 5724–5729.

[38] Chung, S.-H.; Han, P.; Singhal, R.; Kalra, V.; Manthiram, A. Electrochemically stable rechargeable lithium–sulfur batteries with a microporous carbon nanofiber filter for polysulfide. *Adv. Energy Mater.* **2015**, *5*, 1500738.

[39] Li, Z.; Zhang, J. T.; Guan, B. Y.; Wang, D.; Liu, L.-M.; Lou, X. W. D. A sulfur host based on titanium monoxide@carbon hollow spheres for advanced lithium–sulfur batteries. *Nat. Commun.* **2016**, *7*, 13065.

[40] Zhu, L.; Peng, H.-J.; Liang, J. Y.; Huang, J.-Q.; Chen, C.-M.; Guo, X. F.; Zhu, W. C.; Li, P.; Zhang, Q. Interconnected carbon nanotube/graphene nanosphere scaffolds as free-standing paper electrode for high-rate and ultra-stable lithium–sulfur batteries. *Nano Energy* **2015**, *11*, 746–755.

[41] Ma, L.; Zhuang, H. L.; Wei, S. Y.; Hendrickson, K. E.; Kim, M. S.; Cohn, G.; Hennig, R. G.; Archer, L. A. Enhanced Li–S batteries using amine-functionalized carbon nanotubes in the cathode. *ACS Nano* **2016**, *10*, 1050–1059.

[42] Li, G. X.; Sun, J. H.; Hou, W. P.; Jiang, S. D.; Huang, Y.;

Geng, J. X. Three-dimensional porous carbon composites containing high sulfur nanoparticle content for high-performance lithium–sulfur batteries. *Nat*. *Commun*. **2016**, *7*, 10601.

[43] Rehman, S.; Tang, T. Y.; Ali, Z.; Huang, X. X.; Hou, Y. L. Integrated design of MnO_2@carbon hollow nanoboxes to synergistically encapsulate polysulfides for empowering lithium sulfur batteries. *Small* **2017**, *13*, 1700087.

[44] Li, G.-C.; Li, G.-R.; Ye, S.-H.; Gao, X.-P. A polyaniline-coated sulfur/carbon composite with an enhanced high-rate capability as a cathode material for lithium/sulfur batteries. *Adv*. *Energy Mater*. **2012**, *2*, 1238–1245.

[45] Pei, F.; An, T. H.; Zang, J.; Zhao, X. J.; Fang, X. L.; Zheng, M. S.; Dong, Q. F.; Zheng, N. F. From hollow carbon spheres to N-doped hollow porous carbon bowls: Rational design of hollow carbon host for Li–S batteries. *Adv*. *Energy Mater*. **2016**, *6*, 1502539.

[46] Peng, H. J.; Liang, J. Y.; Zhu, L.; Huang, J. Q.; Cheng, X. B.; Guo, X. F.; Ding, W. P.; Zhu, W. C.; Zhang, Q. Catalytic self-limited assembly at hard templates: A mesoscale approach to graphene nanoshells for lithium–sulfur batteries. *ACS Nano* **2014**, *8*, 11280–11289.

[47] Zeng, L. C.; Pan, F. S.; Li, W. H.; Jiang, Y.; Zhong, X. W.; Yu, Y. Free-standing porous carbon nanofibers–sulfur composite for flexible Li–S battery cathode. *Nanoscale* **2014**, *6*, 9579–9587.